Canadian Conference - Pacific Conference on Earthquake Engineering 2023

Vancouver, British Columbia

June 25th – June 30th, 2023

Ensuring Operational Continuity in Hospital Design using State-of-The-Arts Functional Recovery Analyses

Madurapperuma, Manoj[1], Tang, Li Ming[2], Guo, Jack[1*], Zhuang, Yi[2]

[1]Kinetica Risk, Toronto, Canada

[2]EXP, Toronto, Canada

[*] j.guo@kineticarisk.com (Corresponding Author)

ABSTRACT

Incorporating seismic resilience at the early stage of building design can reduce cost and enhance performance while providing better project planning guidance to building owners. However, considering seismic resilience at the early stage of design can be challenging as at this stage, only a preliminary structural design has been carried out, and detailed information about much of non-structural systems is unavailable leading to large uncertainties in cost and scope. This paper describes the performance-based analysis of a new hospital building in southern Ontario at the design and development stage to ensure operational performance under rare seismic events. The lateral force resisting system of the building consists of full height reinforced concrete shear walls, which is a common choice for post-disaster buildings due to their cost-effectiveness and compliance with stringent code requirements for regularity and strength. However, stiff shear wall buildings can attract large accelerations, negatively impacting the operational performance of the building when it houses a large quantity of acceleration sensitive elements. To ensure functional continuity, this study uses the latest methodologies in functional recovery modelling, namely the REDi method and the ATC-138 method, to track the stages of recovery after a design earthquake event. Furthermore, uncertainties in component types, quantities and performance requirements are considered in a series of sensitivity analyses to develop a better understanding of how performance is impacted by these uncertainties in detail at later stages of design. The information generated by this procedure is expected to better support decision-making and planning for the design of new hospitals.

Keywords: Hospitals, functional recovery, FEMA P-58, REDi, ATC-138.

INTRODUCTION

Hospitals constitute a paramount important part of the healthcare system during and following a disaster as it is essential to provide timely treatment and services to life threatening patients in order to minimize fatalities. Post-earthquake disaster studies on major earthquakes such as 2016 Kumamoto earthquake, Japan where regional hospitals were severely affected by leading to loss of more than half the bed capacities forcing evacuation of patients [1]. Similar findings have been reported in 2011 Canterbury earthquake in Christchurch, New Zealand where the Christchurch Hospital sustained structural and non-structural damage, as well as disruption of utility services in both clinical and non-clinical buildings that severely strained the hospital's ability to function at regular capacity [2]. Also, in the 2010 Chile earthquake, four hospitals completely lost their functionality and over 10 hospitals lost almost 75% of their functionality mainly due to damage to sprinkler piping systems [3]. It has been well understood that the widespread damage to non-structural components such as ceiling systems, fire sprinkler pipes, pipe runs for medical gases and steam, and special medical equipment was more disruptive than the localized minor structural damage in code conforming hospital buildings where the stiff shear wall structures tend to attract larger floor acceleration causing damage to these non-structural elements. Many of these elements are critical to functional recovery, and therefore, the operational continuity of a hospital is a major design challenge that needs to be confronted at the onset of the structural design and operational planning process. To overcome most of these challenges, performance-based approach in early stage of design facilitates structural designer to confirm that the design is aligned with the enhance performance objective set out by the owner. The performance-based approach provides a tractable and rational basis to quantify and verify performance objectives expressed in decision-metrics that are better understood by owners.

This study investigates the seismic resilience of a new state of the arts hospital in a large city in southern Ontario to ensure that the design is aligned with the enhance performance objective set out by the owner. The study will be useful to assist the design and development structural design team and the owner in verifying the intended performance level of the complex under the design seismic hazard at the site as prescribed by the Ontario Building Code (OBC) 2019 [4], which is consistent with the hazards in the National Building Code of Canada (NBC) 2015 [5]. The study consists of two distinct objectives: (1) Verify the structural design meets all of the requirements for Immediate Occupancy (IO) structural performance. This is the performance level at which the building retains the full pre-earthquake capacity structurally after experiencing the design earthquake, and (2) Verify that the structural design will enable the entire building system to meet the Operational performance level under the Ontario Building Code (harmonized with the NBC2015) design seismic hazard. This check ensures that the structural system behaves in such a way that so long as the rest of the building systems are designed properly, the entire building is expected to be fully operational following the design earthquake. Both of these objectives are addressed using building models; a structural model that is used for performance-based structural assessment and a performance model that is used for operational assessment.

DESCRIPTION OF MODELING AND ASSESSMENT

Building description and FE models

As shown in Figure 1, the main hospital complex consists of a podium building connected to two 14-storey towers to its east (Tower B) and two 8-storey towers (Tower A) to its west. The Tower B has two wings namely, South wing and North wing, separated by an expansion joint, and therefore, analyze as two separate buildings assuming that these new buildings are adequately separated to avoid seismic pounding. The structural systems of two wings in the Tower B are nearly the same and this section provides details of the structural model including component types, material property estimates and analysis parameters. The main lateral force resisting system (LFRS) consists of cantilever wall in the longitudinal (N-S) direction and a mixture of cantilever and coupled shear wall in the transverse (E-W) direction where the coupling beams are 1.5 m deep and diagonally reinforced. The N-S walls generally have a thickness of 500 mm while the E-W walls generally have a thickness of 700 mm. The gravity system consists of flat slab with gravity columns and column capitals. The relevant acceptance criteria for IO structural performance and Operational performance are listed in Table 1.

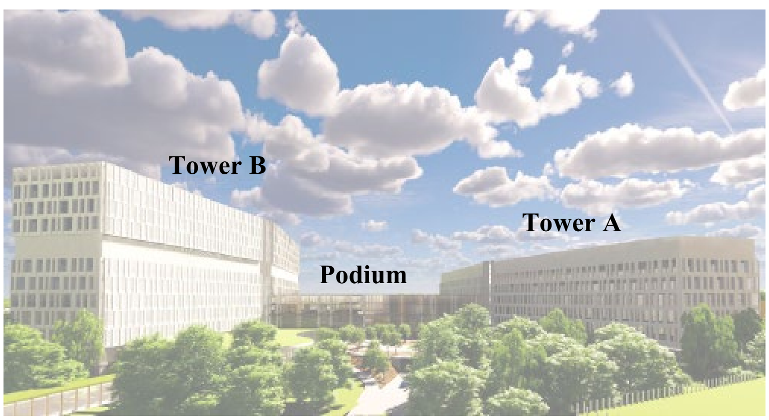

(a)

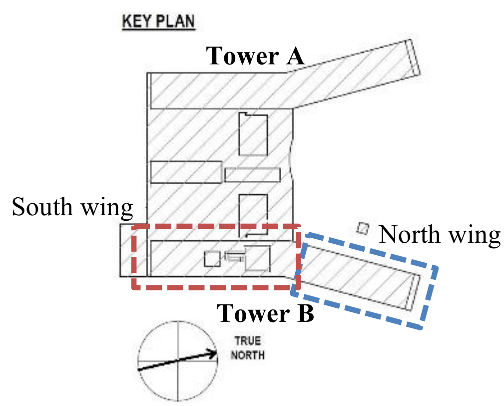

(b)

Figure 1. Details of new hospital complex: (a) Architectural rendering of showing Tower B (left), podium building (centre) and Tower A (right), (b) key plan view showing north and south wings of Tower.

Table 1. Acceptance criteria for the study objectives.

Objective	Acceptance Criteria
Immediate Occupancy Structural Performance	All structural members meet the member-specific immediate occupancy requirements in the ASCE-41-17 [6] under a suite of 11 ground motions scaled in accordance to the requirement of the NBC 2015 structural commentary
Operational Building Performance	The median functional recovery time of the building as evaluated using the FEMA P-58 [7] and REDi [8] and ATC-138[9] methodologies is less than 72 hours (3 days)

A structural model and a performance model are developed for each wing of Tower B to assess the acceptance criteria. Based on the geometry, material properties and loading in an ETABS [10] model, a separate nonlinear model of the structure is developed by translating the model into Perform3D [11]. Prior to building the Perform3D model, a quick check on the relative stiffness ratio between the building and the soil is performed in accordance with the recommendation of the FEMA P-2091 [12] to determine if foundation effects and soil-structural-interaction needs to be considered. It is determined that soil-structure-interaction is deemed not important for this building and a model fixed at the foundation level is judged to be appropriate. In the nonlinear model in Perform3D, the concrete floor slabs are modelled using rigid diaphragm with lumped mass. Both walls and columns are modelled using fibre sections. For walls, end zones area modelled using confined concrete properties while the middle sections are modelled using unconfined concrete properties [13]. Material properties are further modified for regularization of the base hinge region in order to ensure mesh independence [14]. Shear action in both wall and columns are treated as elastic because non-ductile failure modes are assumed to be force-controlled and are designed against at later stages of design, and thus will not govern. Consistent with the requirements of ASCE-41, expected material properties are used to define the deformation-controlled elements. These are obtained by multiplying default material factors in ASCE-41 to the nominal properties. For columns and walls under combined bi-directional bending and axial loads, the concrete and steel fibre materials are defined based on expected properties. Since cracking is automatically accounted for during dynamic analysis by a fibre model, there is no stiffness modification for columns and walls. Link beams and equivalent slab beams are both modelled using concentrated plasticity models. In the case of link beams, separate 2D finite element models were developed for each link beam configurations where the diagonal and vertical distributed reinforcements are modelled explicitly, and reversed cyclic loading protocols were considered to obtain reasonable hysteretic response of these link beams. The resulting hysteretic response is used to calibrate phenomenological shear hinge model in Perform3D. Frame actions from column-slab joints are accounted for by modelling slabs as equivalent beams. Each joint has offsets based on the requirements of ASCE-41 to model the contribution of frame stiffness. The slab sections are cracked according to the recommendations of the PEER TBI [15]. Furthermore, a plastic hinge in the slab beam is introduced at the end of the offset to model the slab rotation with the explicit assumption that column-slab connection region will be reinforced to prevent punching shear failure, and will fully develop the slab beam flexural capacity. The flexural strength of the slab beam is computed using the provisions in CSA A23.3 [16], using expected material properties, and the rotational capacities are modelled as recommended by the ASCE-41. Finally, P-Delta effect is included in the nonlinear model and a combination of modal and Rayleigh damping is used to produce total critical damping of 2.5% for nonlinear dynamic analysis, as recommended in the TBI guideline. Figure 2 shows details of the FE models in Perform3D for South and North wings of the Tower B. Table. 2 shows the first three fundamental modal of the two buildings. It is seen that the lowest eigen mode, that is first fundamental mode is torsion for both the buildings due to long and narrow building foot prints. These modes account for roughly 65% of the seismic mass in both directions.

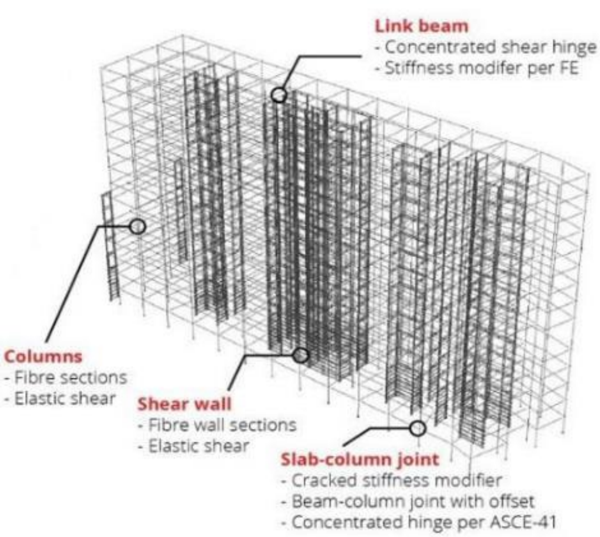

(a)

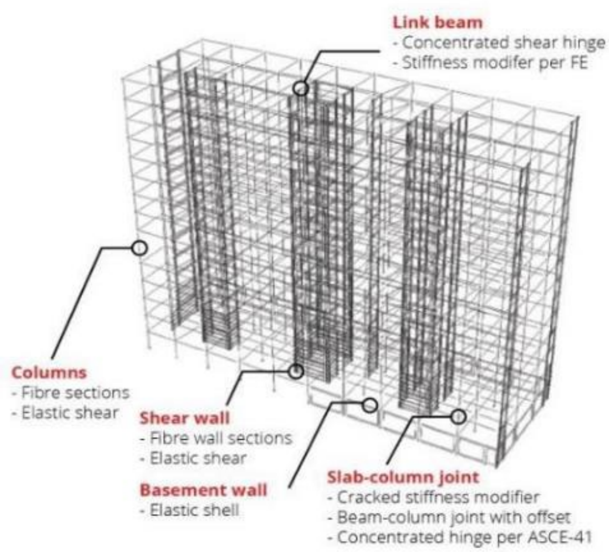

(b)

Figure 2. Details of nonlinear model in Perform3D: (a) South wing, (b) North wing.

Table 2. First three modes of two buildings.

Modes	South wing	North wing
Mode 1	2.25 s (Torsional)	1.95 s (Torsional)
Mode 2	1.90 s (E-W Translational)	1.64 s (N-S Translational)
Mode 3	1.40 s (N-S Translational)	1.56 s (E-W Translational)

To develop further understanding of lateral force resisting mechanism of two buildings, nonlinear static analyses (pushover analysis) are performed in the two principal directions in accordance with the nonlinear static procedure (NSP) described in the

ASCE-41 standard. A lateral force pattern corresponding to the equivalent lateral force in the NBC2015 is used, and the resulting pushover curves (base shear vs roof drift) are shown in Figure 3. The South wing develops approximately 100 MN and 80 MN of base shear strength in the N-S and E-W directions respectively, while the North wing develops approximately 84 MN and 91 MN of base shear strength in the N-S and E-W directions respectively. The nonlinear behaviour of each direction is similar in both buildings, and both directions developed some ductility after global yielding in the lateral force resisting system is reached. In the N-S direction, the behaviour is more ductile due to the high degree of redundancy provided by the walls in the longitudinal direction, as well as additional gravity frames that contribute to the seismic capacity. In the South wing, for N-S direction, yielding first occurs at roughly 0.5% roof drift and the system does not experience a degradation in strength until a roof drift of 3%. On the other hand, the E-W direction exhibits less ductile behaviour. Under a drift level of 0.5% or less, both directions are expected to respond essentially linearly with localized yielding. In the North wing, for N-S direction, yielding first occurs at roughly 0.4% roof drift and the system does not experience a degradation in strength until a roof drift of 3.2% at which point local drift at the emergency level reaches 4%, triggering termination of the pushover analysis. The E-W direction behaviour is similar but it exhibits somewhat less ductile behaviour globally. Yielding first occurs at roughly 0.3% roof drift and the yielding of the three cores are almost simultaneous in this direction. The structure does not experience a degradation in strength until a roof drift of 2.2%, at which point the emergency level storey drift reaches 4%. The reason for the local storey drift to be almost two times the global roof drift is because uneven yielding of the walls at each end of the build leads to twisting of the floor diaphragm which amplifies local drift more than global roof drift. In other words, the building has a torsional sensitivity when the walls are loaded past the elastic limits. Under a drift level of 0.3% or less, both directions are expected to respond essentially linearly with localized yielding.

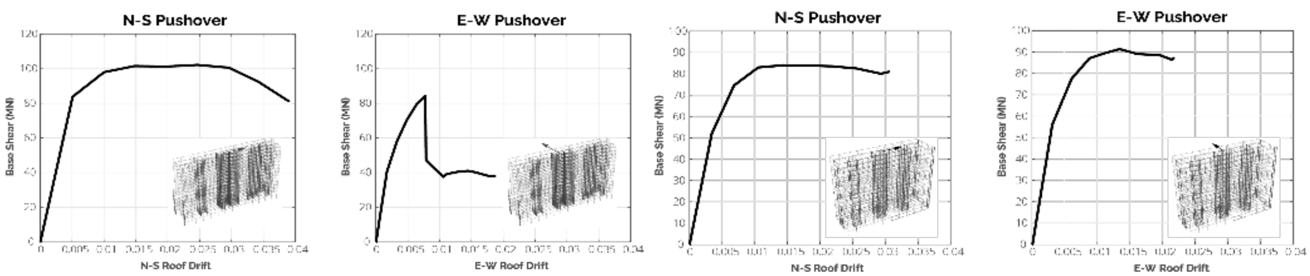

(a) *(b)*

Figure 3. Pushover responses of two building in N_S and E-W directions: (a) South wing, (b) North wing.

Ground motions

Seismic hazard disaggregation data obtained from NRCan [17] at 50 years exceedance probability of 2% is used for the selection of representative seed ground motions. These seed ground motions are then scaled to the appropriate amplitude for each intensity level considered. The hazard disaggregation plot for the site at the 2% in 50 years exceedance probability for spectral acceleration at 2 seconds is presented in Figure 4(a). Following the requirements of the ASCE-41 and the seismic hazard disaggregation of the site, a hazard-consistent suite of ground motions for the explicit evaluation of structural performance is developed for the hospital site using the OBC 2019 seismic hazard. Figure 4(b) shows the log-log plot of the response spectra of 11 scaled ground motions along with their mean and the target spectrum shown in black. This suite of motions consists of 5 recorded ground motions and 6 synthetic ground motions representing large magnitude events where recorded data is extremely scarce. Method A in the NBC 2015 structural commentary J is used as a guide for scaling of ground motions.

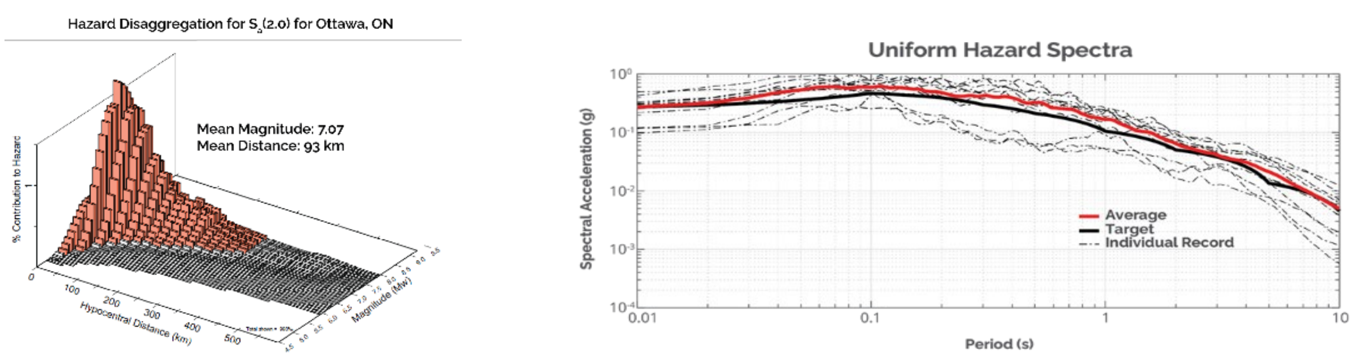

(a) *(b)*

Figure 4. Hazard-consistent suite of ground motions: (a) Seismic disaggregation for the building site for Sa(2.0) at 2% in 50 year hazard intensity, (b) Response spectra for structural assessment using the nonlinear dynamic procedure.

Nonlinear dynamic analysis results

Nonlinear dynamic analysis (NDA) simulates the time-dependent response of the building under a suite of earthquake ground motions scaled to the target spectrum as described above. Structural responses such as drifts, plastic rotations and force demands obtained directly from the analysis are used to determine if code requirements are met, which are based on the IO structural performance objective described by the ASCE-41. Each structural component of the building is designated to be either "force-controlled" or "deformation-controlled". The designation indicates whether a member is brittle, and it fails when the seismic force demand exceeds its strength capacity, or if a member is ductile where failure is caused by the exceedance of its ultimate deformation capacity. In both cases, the seismic force and deformation demands are obtained from the NDA. These seismic demands are then used to compute the demand capacity ratios (DCRs) used for verifying the acceptance criteria. A building meets the IO performance objective if all of its members meet the acceptance criteria corresponding to these performance objectives. This requires that the mean DCR is less than 1.0, and that none of the component fails either by excessive force demand or deformation demand under any of the earthquake.

Figure 5 shows inter-storey drift for two buildings obtained from the NDA for all 11 ground motions. The mean inter-storey drifts in both directions are small due to the low seismic hazard. The mean drifts in both directions are well below 1%, which is drift limit for post-disaster building. In fact, for the South wing, none of the individual record causes storey-drift to be larger than 0.5%. Cross referencing this with the pushover curves in Figure 3, the overall building behaviour in the N-S direction is essentially linear elastic, where localized yielding in some of the walls is expected to occur for the E-W direction. In the case of North wing, only one of the individual records causes inter-storey drift to be slightly larger than 0.5% for N-S direction. Cross referencing this with the pushover curves in Figure 3, very minor localized yielding is expected to occur for N-S direction. However, for the E-W direction, mean of storey-drift is about 0.3% and therefore, yielding is expected in shear wall in this direction for several individual records.

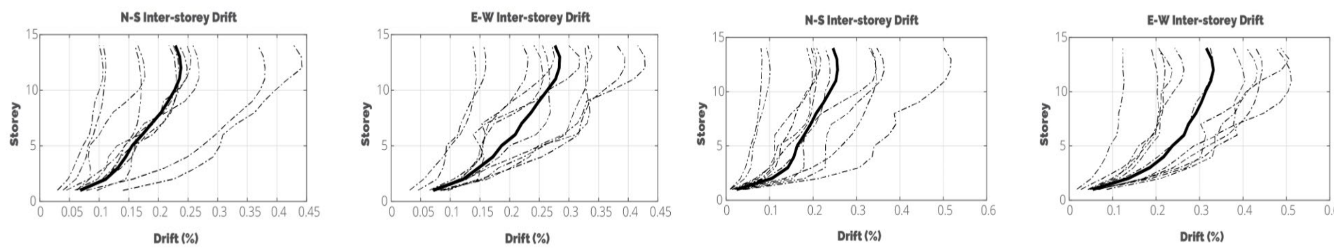

(a) *(b)*

Figure 5. Inter-storey drifts: (a) South wing, (b) North wing.

Figure 6 shows floor accelerations and velocities for two buildings. These values suggest both the building have more 0.5 g floor accelerations for several individual records although mean floor acceleration is about 0.5 g. This means that most of acceleration sensitive components such as fire sprinkler systems, elevators, suspended ceilings, HVACs and piping systems etc., are at a risk of damage or service interruption. For example, based on the FEMA P-58 database, in the case of traction elevators, failure of controller anchorage, machine anchorage, motor generator anchorage, governor anchorage, or rope guard could trigger damage when accelerations are greater than 0.31g. Also, most of piping systems and chillers in HACs trigger damage when accelerations greater than 0.55g and 0.43g, respectively (FEMA P-58). Similarly, mean floor velocities in upper floors are more than 0.5 m/s with individual records exceeding 1 m/s causing velocity sensitive components such as unanchored bookshelves, filling cabinets etc., in upper floors are at high risk of damage. This will affect functional recovery as median velocity thresholds varies from 0.25 m/s to 0.7 m/s for bookcases with six to two shelves.

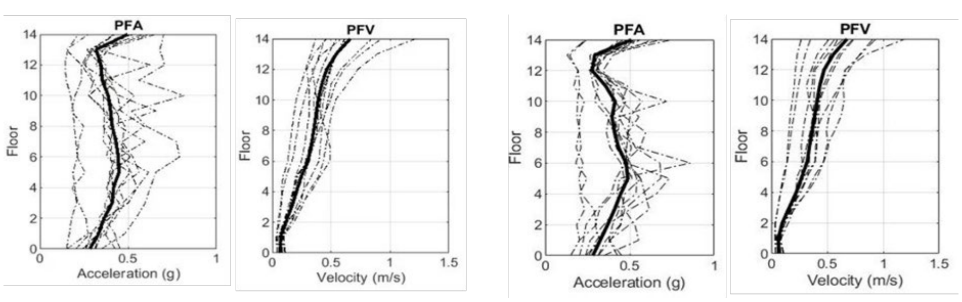

(a) *(b)*

Figure 6. Floor acceleration and velocities: (a) South wing, (b) North wing.

To account for accidental torsion according to ASCE-41, a series of eccentric mass cases are developed for the structural model where the center of mass of the structure are displaced 5% of the building dimension in each direction to envelope the results for force and displacements obtained in the dynamic analysis. Amplification factors are computed using drift and storey shear forces based on eccentric mass cases, and the most critical amplification factors are found to vary between 1.23 - 1.34 and 1.06 - 1.18 along the height of the buildings for South and North wings, respectively. These factors are used to amplify the seismic demands when checking against the acceptance criteria at the component level. The component acceptance checks in the form of demand capacity ratios (DCR) are presented for shear walls and column-slab joints. Note that almost all link beams exhibit very little inelastic shear deformation demand, and they are well within the IO acceptance criteria. In fact, many link beams remain linear elastic.

Figure 7 shows the mean DCR for all shear walls in the buildings against the IO acceptance criteria. The acceptance criteria for IO performance for shear walls is based on inelastic rotation at the wall hinge region, which is measured by a rotational strain gage in the model. It can be seen that the inelastic rotation limits for all walls are well below the IO limit in the ASCE-41, and hence the walls meet IO performance under the design earthquake. In the case of South wing, the worst performing wall is found at the base of the building. However, even these walls reach only 55% of the IO limit for plastic rotation on average. In the case of North wing, the largest DCR occurs at the emergency level (directly above the basement wall) in the narrow walls in the northern frame, where inter-storey drift is amplified due to inherent torsion sensitivity.

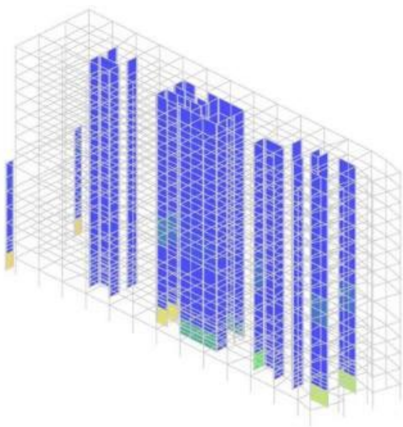

Storey	South Wing (IO)	North Wing (IO)
Storey 12	0.00	0
Storey 11	0.00	0
Storey 10	0.00	0
Storey 9	0.01	0.04
Storey 8	0.00	0.04
Storey 7	0.00	0.07
Storey 6	0.00	0.06
Storey 5	0.08	0.11
Storey 4	0.16	0.26
Storey 3	0.03	0.05
Storey 2	0.03	0.04
Storey 1	0.09	0.05
Emergency	0.08	0.64
Basement	0.55	0.19

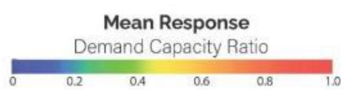

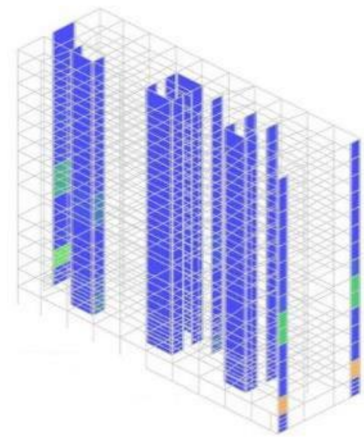

(a) *(b)*

Figure 7. Wall inelastic rotation DCR for IO: (a) South wing, (b) North wing.

Although not designated as part of the main LFRS, the gravity system provides significant contribution to the lateral resistance of the building through frame action in the column-slab joints. The performance of these joints is measured by the inelastic rotation of the column and equivalent beam joint. The DCR for column-slab rotation is summarized in Figure 8 for two buildings. In the case of South wing, a total of 23 slab beams in the building are found to exceed the ASCE-41 IO inelastic rotation limits of 1% plastic rotation, and these are located on the Emergency, 8th to 12th storey. Most of the violations are located within the middle cores where the slab spans are short. The violations in the emergency storey are found in the southern end of the building where there is an opening in the slab. More than half of these joints have DCRs less than 1.1, and only one beam on the emergency storey has a DCR exceeding 1.5. However, in the case of North wing, it can be seen that all column-slab joints are well within the IO acceptance criteria.

Based on the NDA, both the buildings satisfy the IO performance objective for walls and coupling beams. In the case of South wing, failure to meet the IO inelastic rotation limit for equivalent slab beams means that these beams will continue to support gravity and will not post significant falling hazards to occupants however, it affects the functional recovery. Further, the post-earthquake performance of the structure is weakened (very slightly) as compared to its pre-earthquake state. An inspection of the building structural system is likely required, followed by localized repair of the structure before the affected areas can be safely reoccupied. In contrast to the conventional design where engineers ignore the gravity system, the fact that performance-based design requires the consideration of gravity system damage is an important feature for verifying functional continuity of the building which is the main requirement of owners of the hospital facility. Therefore, performance-based seismic assessment at preliminary design and development stage facilitates design engineers to make corrections in the final design as per owners performance objectives.

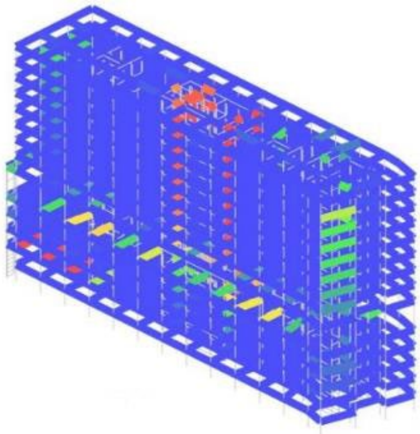

Storey	South Wing (IO)	North Wing (IO)
Storey 12	1.11	0.65
Storey 11	1.31	0.47
Storey 10	1.25	0.42
Storey 9	1.26	0.42
Storey 8	1.24	0.40
Storey 7	1.17	0.38
Storey 6	1.06	0.35
Storey 5	0.96	0.32
Storey 4	0.91	0.27
Storey 3	0.72	0.37
Storey 2	0.71	0.26
Storey 1	0.66	0.22
Emergency	2.82	0.24
Basement	0.41	0.13

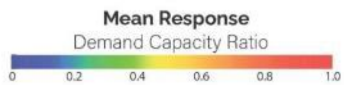

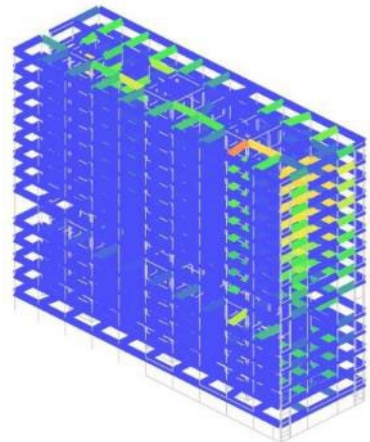

(a) *(b)*

Figure 8. Column-slab inelastic rotation DCR for IO: (a) South wing, (b) North wing.

Building performance model

At the current design and development phase of the building, a performance-based evaluation of the overall building is carried out with the intention of assessing whether the proposed structural system is adequate for enabling the final building to meet the more stringent Operational performance requirement. While the uncertainty is large during the early phase of design, this analysis is an opportunity for providing owners and designers a more comprehensive understanding of the functional performance of the building, as well as important early guidance for meeting the Operational performance requirement in a cost-effective manner as the design progresses. Aside from a structural system that meets the IO performance, an Operational building needs to have power, water, heating and cooling, amongst other building systems required for function. The basis of the detailed building performance assessment procedure employed by this study is the FEMA P-58 standard and its family of methods including the REDi and the ACT-138 methodologies. This analysis uses a building performance model, which captures the occupancy, content, non-structural building systems and operational dependencies of the building. In contrast to a structural analysis, the objective of the building performance assessment is to establish decision-metrics that are required to evaluate the post-disaster damage and functional states through a Monte Carlo risk analysis performed in accordance to the requirements of the FEMA P-58 standard.

At the current design and development stage, the building contents and non-structural design are not finalized. Hence, the performance model used is generated based on provided occupancy data, floor area and relevant building drawings using Kinetica Risk's MARSP platform [18]. Where possible, content quantities are determined by counting individual items or by area/length. Elements that are hidden from view and are not documented in provided reports and drawings are estimated based on building size and occupancy data using the FEMA P-58 normative quantity database, with adjustment done according to the current architectural plans. Relatively large dispersions are used for the quantities of components that are generated from the normative quantity tool to reflect the uncertainty at the design and development phase.

Figure 9 illustrates the performance model used for South wing with some of the building components highlighted, and a similar model is used for North wing. Note that due to the early stage of design, it is not possible to estimate the tenant contents, in this case hospital contents such as medical instruments (e.g., MRI, X-ray), shelved items (e.g., samples, medicines), hazardous contents (e.g., biohazards, chemical tanks). Hence, tenant contents are excluded from the performance analysis, except for large shelves and cabinets which are very common, and are included for the evaluation of safety hazard in case they topple or are damaged. Therefore, the results should be interpreted as a performance evaluation of the building and building systems only. Alternatively, the results can be interpreted as the performance of the entire building when all tenant contents are braced and/or isolated to prevent damage and interruption to function. In terms of recovery, since a hospital is considered an essential facility prior arrangement with contractors and engineers are assumed to be present so post-earthquake recovery can be expedited. Since the building structural system would likely be made to meet IO performance at the design level earthquake, collapse risk is negligeable, and thus is not included in the performance evaluation.

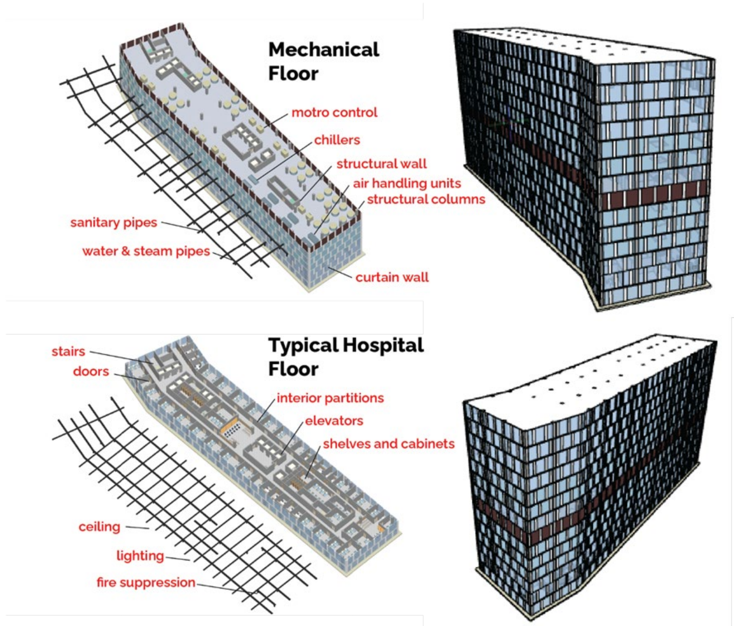

Figure 9. Render of performance model with content based on occupancy (South wing)

Results of building performance assessment

FEMA P-58 analysis

The FEMA P-58 family of method is used to assess the performance of the building. The FEMA P-58 analysis itself is used to analyze the damage and loss associated with the code level earthquake, and it forms the basis for subsequent recovery analysis. In this analysis, 5000 simulations are performed at the deign level seismicity that models the damage throughout the building, which is the basis for determining loss and operational disruption. It is found that mean direct loss values are \$ 2.79M and \$1.92M for South and North wings, respectively. The losses are equal to the total cost of repairing damaged elements, and are direct measures of financial impact useful for the management of financial risk associated with earthquake damage. Environmental impacts reported by the analysis are the embodied green house gas (GHG) emissions expressed in tonnes of equivalent CO2, as well as energy consumed in the aforementioned repair activities. The mean GHG values are 478 tCO_2e and 365 tCO2e for South and North wings respectively. These are useful for planning life-cycle costs of the hospital and assessing the overall cost-benefits of design decisions when environmental and sustainability metrics are involved. A breakdown of damaged components in terms of the mean direct loss, embodied carbon and energy cost is shown in Figure 10 for two buildings. Each slice of the pie chart represents the contribution of the element to the average building loss at the design seismic hazard level. In this case, the financial cost drivers are interior partition, mechanical and structural repair and HVAC repair. The cost drivers are similar from an embodied carbon and energy perspectives, with the exception of pipe repair, which is a driver for energy consumption, while being only a minor contributor to financial loss and CO_2 emissions. The cost drivers are not surprising since stiff shear wall structures tend to attract larger floor acceleration throughout the building, which is the main cause of damage to non-structural elements such as elevators, suspended piping, ducting and anchored equipment. Many of these elements are critical to function recovery, and their impact is evaluated by recovery assessments using REDi and ATC-138 methodologies.

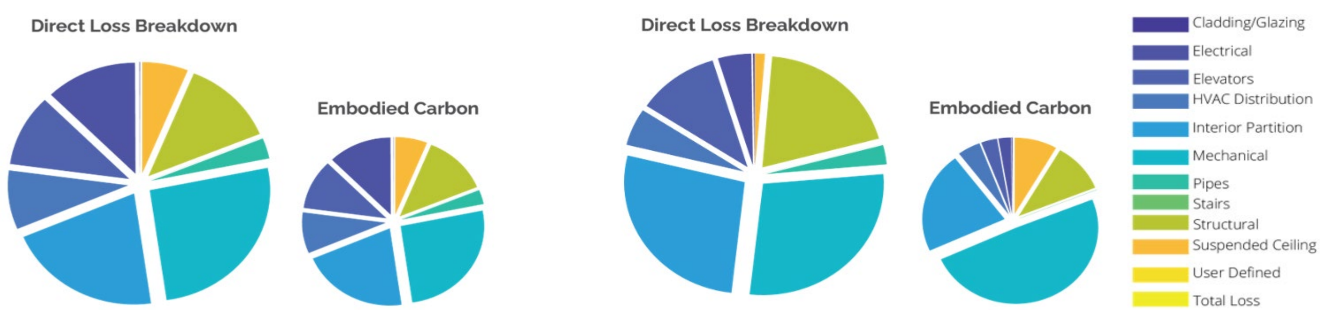

(a) *(b)*

Figure 10. Breakdown of factors contributing to mean direct loss: (a) South wing, (b) North wing.

REDi functional recovery assessment

The REDi method is the most common method for evaluating post-earthquake recovery time built on the FEMA P-58 analysis. The method reports three different recovery times, namely, reoccupancy time, functional recovery time and full recovery time. The reoccupancy time is defined as the time elapsed before the building recovers to a state where all of its area can be safely occupied (no collapse and no falling hazard) by a human occupant. The functional recovery time is the time elapsed before the building recovers all of its pre-earthquake function. Finally, the full recovery time is the time elapsed before every single element in the building recovers to the pre-earthquake state. These three recovery states are increasingly more stringent, and each successive recovery state requires additional elements to be repaired. According to the REDi methodology, it is found that 68 and 67 days are required for the base case South and North wings, respectively to reach functional recovery under the median scenario which is much longer than the Operational performance target of 72 hours, or 3 days. Hence, the building does not meet the Operational performance criteria in Table 1 above according to the REDi procedure. Figure 11 shows the histogram (probability vs recovery time range) of functional recovery times and a breakdown of the factors contributing to the functional recovery times for South and North wings. It can be seen from the histogram that most of the 5000 simulations have recovery times between approximately 40 days to 80 days, although there is a group of cases that have only a few days of recovery time or less. It is seen that while most of the downtime is caused by delays for mobilizing engineers and contractors to complete repair work, the actual demand for mobilizing contractor comes from damage in elevator, electrical, mechanical, and interior system repair times. It can be seen from the median scenario that despite not contributing much to the time for completing functional repair, piping system damage is actually the most ubiquitous throughout the building in the median case. This is because the large quantity of pipes makes piping damage common, although replacing the pipe coupler or brace is typically very inexpensive. However, they can make the building non-functional when they leak or are causing falling hazard to the occupants below. On the other hand, while mechanical and elevator repair contribute much larger portion to the recovery time due to their more complex and labour-intensive repair, they are only concentrated at the base and the mechanical floor.

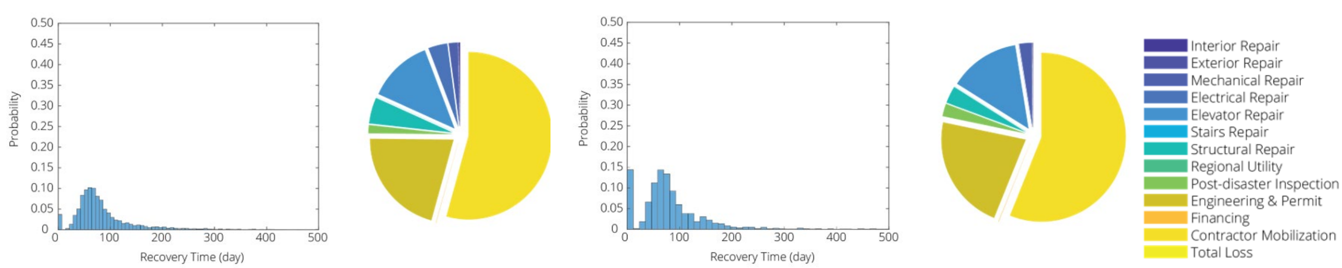

(a) *(b)*

Figure 11. Functional recovery time by histogram and breakdown of contributing factors: (a) South wing, (b) North wing.

Figure 12 provides the recovery schedules in the form of a repair Gantt chart from a selected realization for South and North wings. These plots not only show where repair needs to be done, they also plot the associated delays with post-disaster inspection, financing, as well as engineering and contractor mobilization. These scenarios represent well the type of damage likely to be found for a functional recovery of around 70 days. In some cases, the damage is found in a multitude of functionally-critical elements including elevators, interior finish (includes water pipes), HVAC distribution and electrical elements. In other cases, the elevators seem to be the bottleneck for recovery along with minor interior finish repair work, which includes piping repair. These plots suggest that targeting the interior piping and elevators have the best chance of reducing the median recovery time.

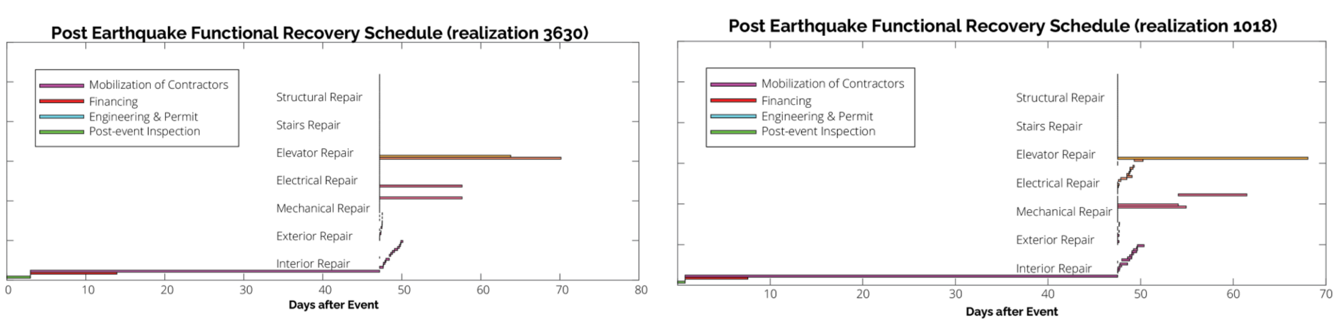

(a) *(b)*

Figure 12. Functional recovery Gantt charts: (a) South wing, (b) North wing.

Furthermore, reducing piping damage is more cost effective compared to reducing elevator damage because piping performance can be increased by improving engineering detailing of pipe anchorages and connections, while it is difficult to introduce design changes to elevators. Assuming that the pipe anchorage will be addressed during the detailed mechanical electrical and plumbing (MEP) design phase, a revised performance model of the building with "enhanced pipe design" is analyzed. In this model, hot and cold water pipes and anchorages are assumed to be upgraded to resist a larger acceleration. In the case of South wing, the enhanced pipe design scenario is able to achieve zero functional recovery time under the median scenario. It is found that the probability of having zero recovery time is actually barely over 50%, which means the criterion on the median recovery time being less than 72 hours is met by a very small margin. However, in the case of North wing, enhancing the piping design is not enough to meet the Operational target since the median recovery time only reduced slightly from the base case. Despite this small reduction in median recovery, it is found that there is actually a very substantial increase in the probability of having an immediate recovery, which is 14% in the base case, to 42% in the enhanced design. Many of the cases that previously had recoveries times between roughly 50 to 120 days have been reduced to zero, which indicates that "hardening" piping design is an effective means for preventing functional disruption for the North wing. For both South and North wings, after addressing the damage in the pipe and anchorages, the relative contribution of elevator repair is now much larger. At the same time, contractor mobilization is less of a bottleneck because mobilization time for the plumbing trade is eliminated. Since the performance criterion is barely met for South wing and not sufficient for North wing by the REDi analysis, an alternative procedure for functional recovery within the FEMA P-58 family of methods is used to gain additional information and assurance on the functional recovery.

ATC-138 functional recovery assessment

The ATC-138 methodology is a newer and more comprehensive method for evaluating functional recovery time introduced by FEMA in 2021 as part of the FEMA P-58 family of methodologies. ATC-138 analysis can be better tailored to individual facilities and is more suitable for functional continuity planning at latter stages of design where detail information about the building system is available. The ATC-138 method also relaxes several important assumptions in the REDi that is well-recognized to result in longer recovery times than observed in practice, such as non-zero tolerances for building system damage due to temporary reactionary measures and built-in redundancies in many of the building systems by design. Since the REDi results shows that these buildings barely meets or insufficient for the Operational performance when piping vulnerabilities are addressed, having both REDi and ATC-138 functional recovery analyses can provide a more robust basis for understanding functional recovery for operational continuity planning. Default ATC-138 tolerances for all building systems are used for this analysis since its intention is still to perform a preliminary evaluation of the current structural design for achieving an Operational building. Figure 13 compares the histogram of the functional recovery times for base building and enhancement in pipe design.

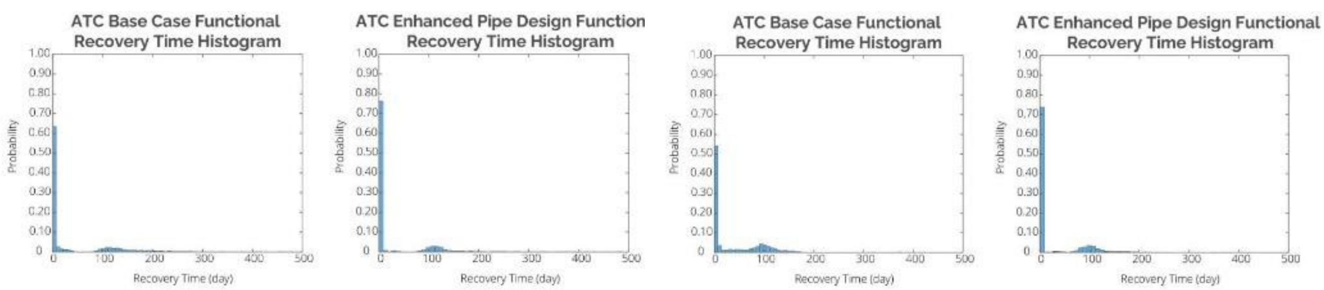

(a) *(b)*

Figure 13. ATC-138 based functional recovery time by histogram: (a) South wing, (b) North wing.

As shown in Figure 13, even without the enhancement in pipe design, using the ATC-138 method, the two buildings almost meets the Operational performance requirement of functional recovery within 72 hours (3 days). With the enhancement in the pipe design, the Operational performance objective is met. The histograms of the ATC-138 functional recovery time show the most likely outcome for both buildings are zero, or a few days of functional recovery time (first bin covers a range of recovery times up to a few days). The second most likely outcome would be having downtime of roughly 80 to 120 days. Fixing the pipes does not change the pattern of the histogram distribution since these scenarios are caused by damage in unrelated components, such as elevator and HVAC equipment. Unlike REDi which uses component damage as direct indicators of building function, ATC-138 uses building services and building system damages. To illustrate the system functional states within the building, the level of recovery for the median scenario broken down to each building service is shown in Figure 14 for both the base case and the enhanced pipe design case.

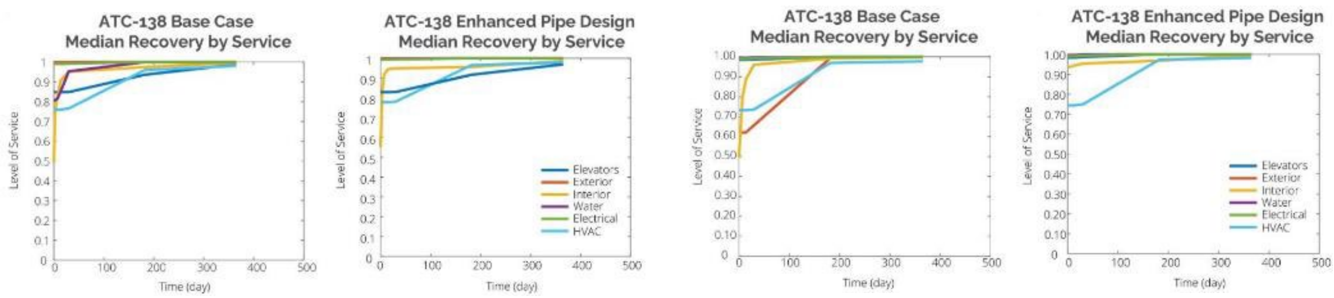

(a) *(b)*

Figure 14. Comparison of ATC-138 median scenario system recovery trajectory: (a) South wing, (b) North wing.

The recovery trajectories of six building services are tracked by the ATC-138 analysis. Every service is delivered by a collection of building components, and a given building component may be involved in delivering multiple services. Note that piping elements affect both the interior system (pipe or anchorage falling, leaks, and other damage to the ceiling and partition), and water system (distribution of water from municipal source throughout the building). It can be seen that the primary difference in the median scenario between the two cases is the faster recovery of water system in the latter. The delivery of water throughout the building due to piping and anchorage damage is not severely impacted since the damages are small. In the base case, damaged building envelop also plays a role in delaying functional recovery. This system is not damaged in the median case of the enhanced pipe design. Note that while enhancing the piping and anchorage has no impact on the exterior system, it reduces functional recovery time for the cases that are governed by piping damage which in turn changes the median scenario. This is why exterior damage no longer plays a role in the median scenario after piping design is enhanced. Since the criteria for Operational performance depends only on the median scenario, enhancing the design of the piping system alone is sufficient to meet the performance objective in this case. Also, there is a comparable impact to the HVAC systems in the building for both cases. One source of damage is equipment malfunction or physical damage in mounted equipment, such as chillers and air handling units, at the mechanical floor. Another source is the HVAC distribution damage throughout the building. In this case, the reduction in the level of service of the system is less than the ATC-138 systems default tolerance for HVAC systems, which are typically are designed to be redundant. When detailed design of the HVAC system is available, this tolerance may be adjusted to reflect the actual design intent if necessary. As shown in Figure 14, not all building systems achieve 100% of the pre-earthquake service immediately after the earthquake. Yet, due to the tolerance allowed by the ATC-138 methodology, the building is still considered functional. At a later stage of design where detailed information pertaining to the building system components is available, the method can be refined to better support functional continuity planning.

Seismic risk assessment is performed in accordance with performance-based assessment standards specified above. Where information is not available to fully define the building contents, engineering assumptions are made based on applicable codes and accepted standards of practice. For example, the use of normative quantity generator for developing building contents would only offer approximate performance assessment. Detailed building information models or databases can be used at a latter stage to capture the specific contents in the buildings. The present analysis makes reasonable assumptions about tolerances of each building system (e.g. number of elevators that need to be functional, number of tolerable failures in HVAC equipment, fraction of damaged partitions etc.). These need to be discussed with the operational team and business continuity team at latter design stage to investigate the impact of uncertainties around these limits. The performance models do not include hospital contents such as medical instruments (e.g., MRI, X-ray), shelved items (e.g., samples, medicines), hazardous contents (e.g., biohazards, chemical tanks) due to the lack of such information. However, by working with the site planning team (people who determine the usage and occupancy of each floor area), a more detailed analysis at a latter stage can be performed to provide better assessment and provide more specific scenarios for contingency planning.

CONCLUSION

Performance-based structural and operational seismic risk assessment provide early advice to building owners in order to ensure functional performance requirements are met in the building design. It also provides a basis for understanding expected building behaviour under major earthquakes and assists contingency planning and operational resilience. The paper presents results of performance-based operational continuity study of a new hospital building in southern Ontario using state-of-the-arts functional recovery analyses. The target building of the hospital complex has two reinforced concrete shear wall structures namely, South and North wings separated by a seismic joint. The scope completed include a nonlinear dynamic analysis based structural assessment for verifying IO performance as per the requirements of the ASCE-41 code, as well as a FEMA P-58 based verification of the building Operational performance objective. The purpose of this work is to assist structural designer in establishing a preliminary structural design that aligns with the ultimate Operational performance goal under the design seismic hazard at the design and development stage. As such, it was found that the South wing has isolated inadequacies in column-slab joints that have inelastic rotation limits exceeding the IO limits in the ASCE-41. However, only very few of these joints were identified and they may be easily remedied during the final structural design stage to meet IO performance. In the case of North wing, the building structural system is found to meet ASCE-41 requirements for IO, provided that force-controlled failures in all structural elements are avoided by design at a later stage, as is typically done.

As for the overall building performance, the FEMA P-58 and functional recovery analyses performed in accordance with the REDi and ATC-138 methodologies shows that most of the damage that may cause functional disruption occurs in acceleration sensitive elements such as mounted mechanical equipment, plumbing elements, and elevators. Specifically, the median functional recovery time is found exceed the Operational limit under the REDi analysis but satisfies the limit under the ATC-138 analysis which incorporates more realistic assumptions about system tolerances due to built-in redundancy and reactionary measures that can be taken post-earthquake. Given the latter is a more realistic assessment of functional recovery, the current structural system design is likely able to allow the overall building to meet Operational performance. A potential remedy involving enhancing the water pipe anchorage and connection design using a performance-based approach is also investigated. While the exact scope of this cannot be determined without the details of the plumbing system, it would involve designing piping connection and anchorage elements using acceleration demands obtained from a similar analysis as the one presented in this study, rather than just following the minimum code prescriptive requirement. By doing this to reduce damage in the plumbing system, the building can substantially increase the likelihood of meeting the Operational performance target. In either case, a performance-based verification of the overall building performance is recommended when details of the final structural and non-structural design are available.

ACKNOWLEDGMENTS

The authors would like to express special appreciation to the HDR architectural team, project prime consultant, for their tremendous support and professional guidance provided throughout the entire study. HDR team's collaboration and assistance were essential for the success of this study.

REFERENCES

[1] Achour, N. and Miyajima, M. (2020). “Post-earthquake hospital functionality evaluation: The case of Kumamoto Earthquake 2016”. Earthquake Spectra, 36(4), 1670-1694.

[2] McIntosh, J.K., Jacques, C., Mitrani-Reiser, J., Kirch, T.D., Giovinazzi, S. and Wilson, T.M. (2012). “The impact of the 22nd February 2011 earthquake on Christchurch Hospital”. NZSEE Conference.

[3] Miranda, E., Mosqueda, G., Retamales, R. and Pekcan, G. (2012). “Performance of nonstructural components during the February 27, 2010 Chile Earthquake”. Earthquake Spectra, 28(suppl1), 453–471.

[4] Ontario Building Code (OBC 2019), Containing the Building Code Act, 1992, and O. Reg. 332/19.

[5] National Research Council of Canada (NBC 2015), Structural Commentaries (User’s Guide – NBC 2015: Part 4 of Division B), Ottawa, Canada.

[6] ASCE standard (ASCE-41 2017), Seismic evaluation and retrofit of existing buildings, ASCE/SEI, 41-17, American Society of Civil Engineers, Reston, Virginia, 2017.

[7] Applied Technology Council (FEMA P-58 2018), Seismic performance assessment of buildings, Redwood City, CA.

[8] REDi Rating System (2013), Resilience-based Earthquake Design Initiative for the Next Generation of Buildings, ARUP.

[9] Applied Technology Council (ATC 138), Seismic Performance Assessment of Buildings Vol 8 – Methodology for Assessment of Functional Recovery Time, 2021, Redwood City, CA.

[10] Computer and Structures (2022) ETABS V19. CSI America.

[11] Computer and Structures (2022) Perform3D V7.0. CSI America.

[12] Applied Technology Council (FEMA P-2091 2020), A Practical guide to soil-structure interaction, Redwood City, CA.

[13] Saatcioglu, M. and Razvi, S. (1992), “Strength and ductility of confined concrete”, Journal of Structural Engineering, ASCE, 118(6), 1590-1607.

[14] Lowes, L.N., Lehman, D.E. and Baker, C. (2018), “Recommendation for modeling the nonlinear response of slender reinforced concrete walls using Perform-3D”, SEAOC 2016.

[15] PEER TBI (2017), Tall buildings initiative, Guidelines for performance based seismic design of tall buildings. 2.03. Pacific Earthquake Engineering Research Center (PEER), Berkeley, CA.

[16] Canadian Standard Association CSA (2019), Design of concrete structures, *CAN/CSA-A23.3:19*, CSA Group, 178 Rexdale Boulevard, Toronto, ON.

[17] Natural Resources Canada (NRCan 2022), Request of seismic hazard disaggregation, Kinetica Risk, July 2022.

[18] Kinetica Risk MARSP (2022), Multi-hazard asset resilience strategic planner, V.2.0, Kinetica Risk.